Electronic Supplementary Material (ESI) for Physical Chemistry Chemical Physics.


# Supplementary Information for "Effect of water on the electroresponsive structuring and friction in dilute and concentrated ionic liquid lubricant mixtures"

Georgia A. Pilkington[a,*], Rebecca Welbourn[b], Anna Oleshkevych[a], Seiya Watanabe[a,†], Patricia Pedraz[a], Milad Radiom[a], Sergei Glavatskih[c,d] and Mark W. Rutland[a,e,*]

*[a]Division of Surface and Corrosion Science, School of Engineering Sciences in Chemistry, Biotechnology and Health, KTH Royal Institute of Technology, SE-100 44 Stockholm, Sweden. [b]ISIS Facility, Rutherford Appleton Laboratory, STFC, Chilton, Didcot, OXON OX11 0QX, UK. [c]System and Component Design, Department of Machine Design, KTH Royal Institute of Technology, SE-100 44 Stockholm, Sweden. [d]Department of Electrical Energy, Metals, Mechanical Constructions and Systems, Ghent University, B-9052 Ghent, Belgium. [e]Surfaces, Processes and Formulation, RISE Research Institutes of Sweden, SE-100 44 Stockholm, Sweden.*

*[*]Correspondence: georgiap@kth.se or mark@kth.se*

*[†]Current address: Tokyo University of Science, Department of Mechanical Engineering, 6-3-1 Niijuku, Katsushika-ku, Tokyo 125-8585, Japan*

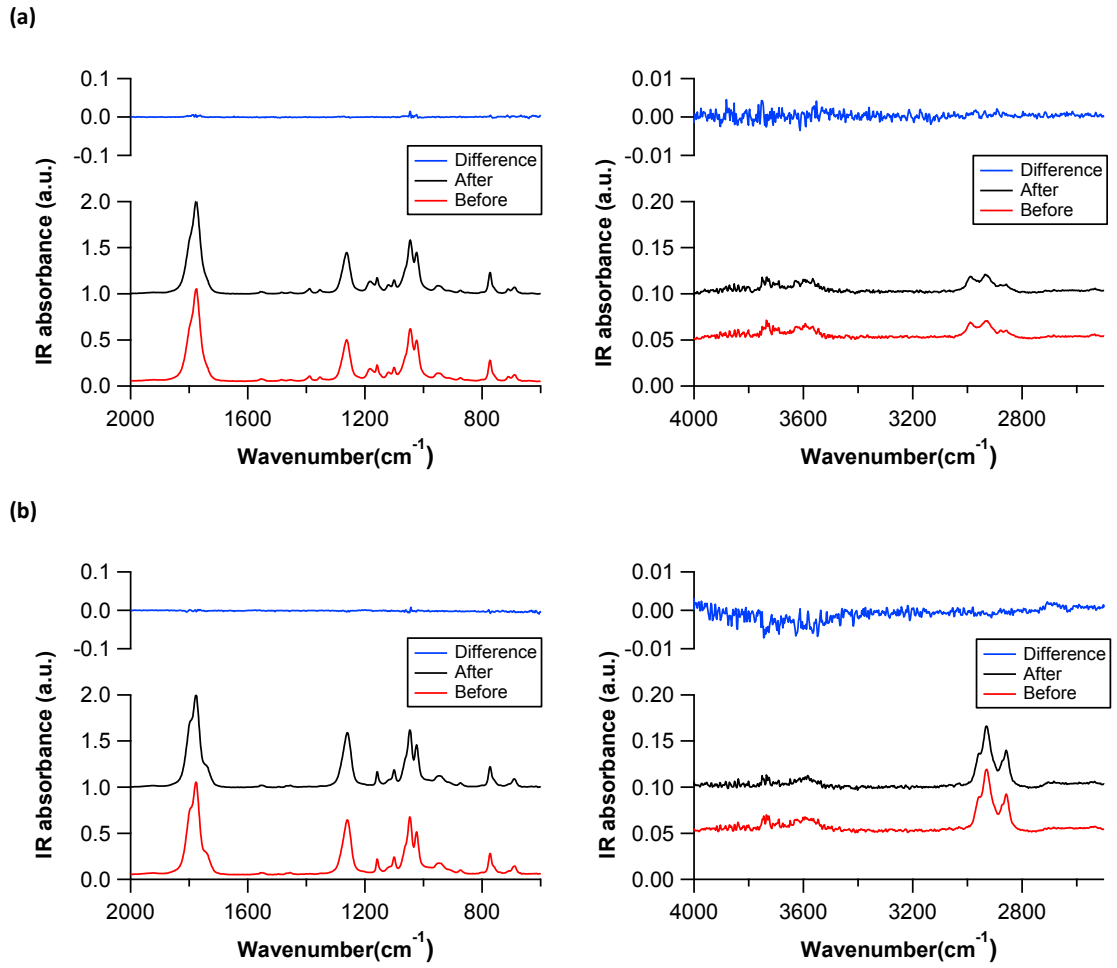


**Figure S1.** Comparison of IR spectra of **(a)** 5% $[P_{6,6,6,14}][BMB]$ + 0.5% w/w $D_2O$ and **(b)** 20% $[P_{6,6,6,14}][BMB]$ + 1% w/w $D_2O$ solutions before (red lines) and after (black lines) NR measurements over the wavelength ranges of 600-2000 $cm^{-1}$ and 2500-4000 $cm^{-1}$. No detectable changes were observed, as demonstrated by the difference in the spectra shown above (blue lines).

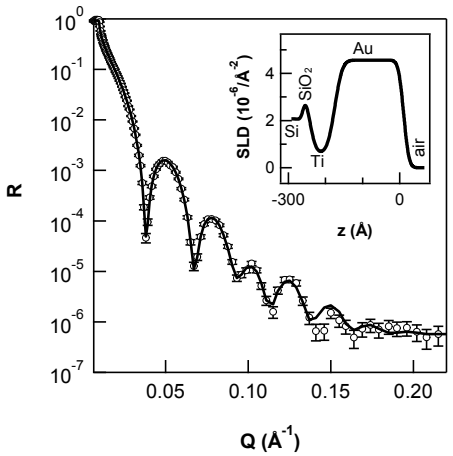


**Figure S2**. Example of the normalised reflectivity for a gold electrode in air. The symbols represent experimental data, while the solid lines represent fitted scattering length density (SLD) model fits to the data. The inset shows the corresponding SLD profile. This block was used for NR measurements in 20% $[P_{6,6,6,14}][BMB]$ with 0.5% $D_2O$.

**Table S1.** Example fitted parameters for a gold electrode in air corresponding to the model fit (solid line) presented in Figure S2.

| Layer | Thickness (Å) | Roughness (Å) | SLD (×10$^{-6}$Å$^{-2}$) |
|---|---|---|---|
| Au | 185.0 | 11.2 | 4.56 |
| Ti | 68.3 | 16.2 | 0.62 |
| $SiO_2$ | 16.9 | 13.5 | 3.47 |
| Si | ∞ | 6.3 | 2.07 |

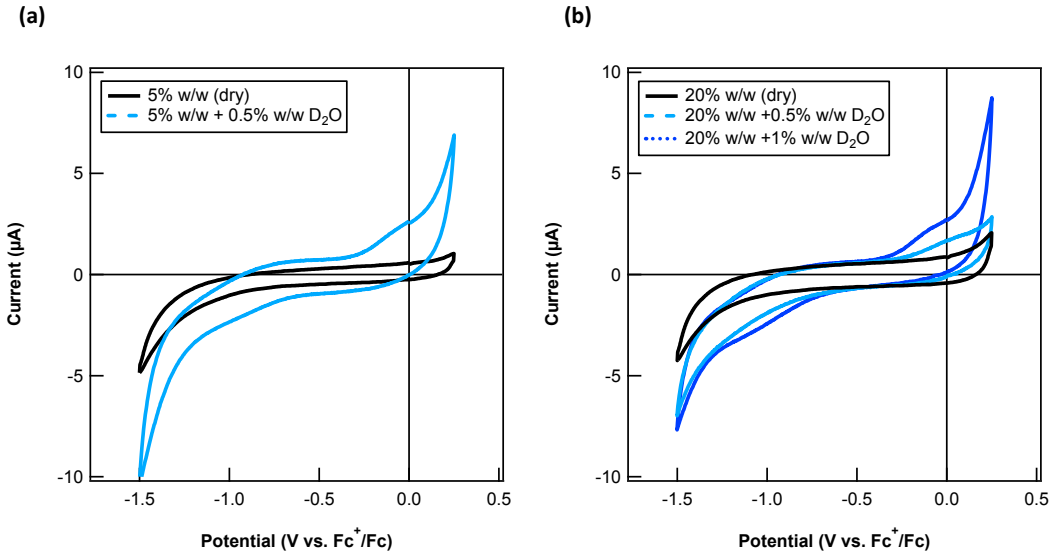


**Figure S3.** Representative cyclic voltammograms of current versus potential for **(a)** 5 and **(b)** 20% w/w solutions of $[P_{6,6,6,14}][BMB]$ in PC with different $D_2O$ concentrations collected at a sweep rate of 10 mV/s.

**Table S2.** Surface charge densities calculated for different applied potentials for 5% w/w $[P_{6,6,6,14}][BMB]$ + 0.5% w/w $D_2O$ after 30 minutes stabilisation period prior to NR measurements.

| Measurement | Potential (V) | Surface Charge (C) | Surface charge density ($\mu C/cm^2$) |
|---|---|---|---|
| 1 | 0 | 0.00105 | 59.69 |
| 2 | -1000 | -0.00379 | -215.09 |
| 3 | 250 | 0.00164 | 93.09 |
| 4 | -500 | -0.00086 | -48.69 |
| 5 | 0 | 0.00017 | 9.50 |
| 6 | -1500 | -0.00663 | -375.88 |
| 7 | 0 | 0.00059 | 33.72 |

**Table S3.** Surface charge densities calculated for different applied potentials for 20% w/w $[P_{6,6,6,14}][BMB]$ + 0.5% w/w $D_2O$ after 30 minutes stabilisation period prior to NR measurements.

| Measurement | Potential (V) | Surface Charge (C) | Surface charge density ($\mu C/cm^2$) |
|---|---|---|---|
| 1 | 0 | 0.00028 | 16.02 |
| 2 | -1000 | -0.00544 | -308.52 |
| 3 | 250 | 0.00155 | 87.59 |
| 4 | -500 | -0.00040 | -22.61 |
| 5 | 0 | 0.00015 | 8.45 |
| 6 | -1500 | -0.00823 | -466.55 |
| 7 | 0 | 0.00108 | 60.95 |

**Table S4.** Surface charge densities calculated for different applied potentials for 20% w/w $[P_{6,6,6,14}][BMB]$ + 1% w/w $D_2O$ after 30 minutes stabilisation period prior to NR measurements.

| Measurement | Potential (V) | Surface Charge (C) | Surface charge density ($\mu C/cm^2$) |
|---|---|---|---|
| 1 | 0 | 0.00045 | 25.27 |
| 2 | -1000 | -0.00308 | -174.67 |
| 3 | 250 | 0.00158 | 89.83 |
| 4 | -500 | -0.00100 | -56.66 |
| 5 | 0 | 0.00031 | 17.39 |
| 6 | -1500 | -0.00573 | -324.56 |
| 7 | 0 | 0.00088 | 49.92 |

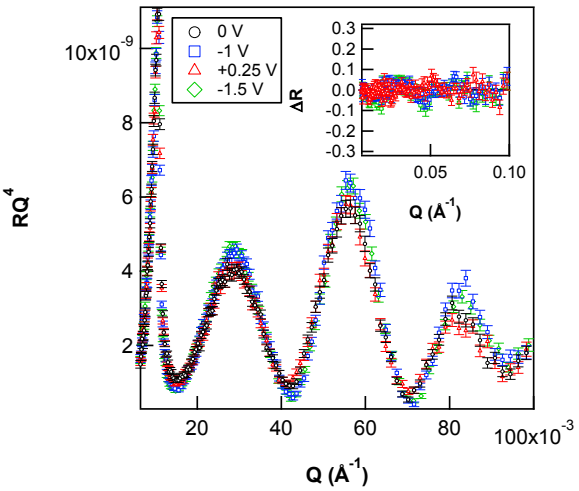


**Figure S4.** Fresnel normalised reflectivity for 20% w/w [$P_{6,6,6,14}$][BMB] in PC with 1% w/w D2O at gold electrode surface for different applied potentials (indicated in the legend). The inset shows an asymmetry plot $\Delta R = [R^V(Q)-R^0(Q)]/[R^V(Q)+R^0(Q)]$ highlighting the changes in the non-zero potential reflectivities ($R^v$) with respect to those at 0 V ($R^0$).

**Table S5.** Fitted parameters obtained from reflectivity curves 5% w/w [$P_{6,6,6,14}$][BMB] + 0.5% w/w $D_2O$ solution at different applied potentials.

| Potential (V) | Layer | Thickness (Å) | Roughness (Å) | SLD (10 $^{-6}$Å$^{-2}$) |
|---|---|---|---|---|
| 0 | 1 | 30.2 | / | 3.25 |
| | 2 | 26.9 | 3.98 | 4.15 |
| | Bulk | ∞ | 9.37 | 4.5 |
| -1 | 1 | 34.6 | / | 2.93 |
| | Bulk | ∞ | 15.6 | 4.5 |
| +0.25 | 1 | 30.3 | / | 3.13 |
| | 2 | 29.8 | 14.7 | 4.12 |
| | Bulk | ∞ | 13.2 | 4.5 |
| -1.5 | 1 | 39.8 | / | 2.82 |
| | Bulk | ∞ | 17 | 4.5 |

**Table S6.** Fitted parameters obtained from reflectivity curves 20% w/w $[P_{6,6,6,14}][BMB]$ + 0.5% w/w $D_2O$ solution at different applied potentials.

| Potential (V) | Layer | Thickness (Å) | Roughness (Å) | SLD ($10^{-6}$Å$^{-2}$) |
|---|---|---|---|---|
| 0 | 1 | 14.9 | / | 2.62 |
| | 2 | 15.3 | 2.85 | 4.9 |
| | 3 | 6.92 | 3.43 | 2.76 |
| | Bulk | ∞ | 3.34 | 4.56 |
| -1 | 1 | 5 | / | 1.61 |
| | 2 | 37.7 | 2 | 3.77 |
| | Bulk | ∞ | 11.9 | 4.56 |
| +0.25 | 1 | 5 | / | 2.01 |
| | 2 | 33.5 | 2 | 3.94 |
| | Bulk | ∞ | 12 | 4.56 |
| -1.5 | 1 | 5 | / | 1.31 |
| | 2 | 32.7 | 2 | 3.64 |
| | Bulk | ∞ | 10 | 4.56 |

**Table S7.** Fitted parameters obtained from reflectivity curves 20% w/w $[P_{6,6,6,14}][BMB]$ + 1% w/w $D_2O$ solution at different applied potentials.

| Potential (V) | Layer | Thickness (Å) | Roughness (Å) | SLD ($10^{-6}$Å$^{-2}$) |
|---|---|---|---|---|
| 0 | 1 | 10.1 | / | 1.87 |
| | 2 | 41 | 3.1 | 4.1 |
| | Bulk | ∞ | 1 | 4.52 |
| -1 | 1 | 13.9 | / | 1.82 |
| | 2 | 33.3 | 2 | 3.88 |
| | Bulk | ∞ | 4.56 | 4.52 |
| +0.25 | 1 | 12.9 | / | 1.98 |
| | 2 | 15.2 | 2.83 | 4.47 |
| | 3 | 15.1 | 5 | 3.48 |
| | Bulk | ∞ | 10 | 3.48 |
| -1.5 | 1 | 5 | / | 0.5 |
| | 2 | 36.2 | 2.4 | 3.69 |
| | Bulk | ∞ | 13.8 | 4.52 |

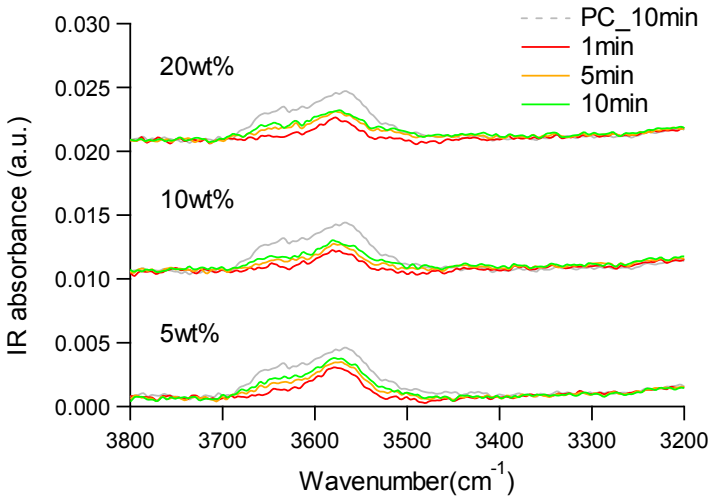


**Figure S5.** IR spectra of different concentrations of $[P_{6,6,6,14}][BMB]$ in PC solution upon exposure to ambient air at a relative humidity (R.H.) of 25% and at 20°C. The solutions reach saturation after 10 minutes. A spectrum for a pure PC solution after 10 minutes exposure is shown for comparison. The water content after 10 minutes was estimated to be: 0.23% w/w in pure PC, and 0.14 and 0.08% w/w for 5 and 20% w/w $[P_{6,6,6,14}][BMB]$ in PC, respectively.

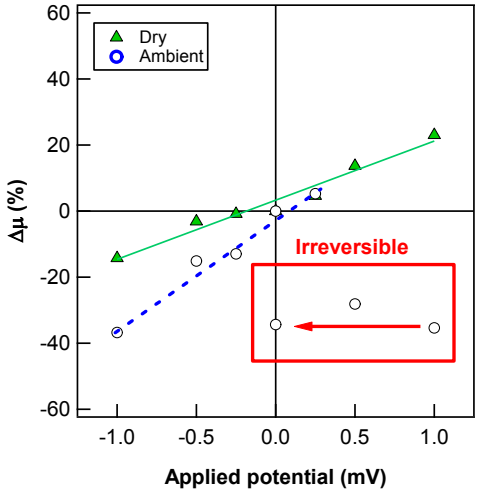


**Figure S6.** Friction coefficient μ as a function of applied potential during loading for dry and ambient conditions at a velocity of 6 μm/s for wider positive potential range than shown in the main manuscript. The observed changes in μ for +0.5 V and +1 V in ambient conditions are markedly different to that observed under dry conditions, which shows a systematic increase in μ with increasingly positive potential up to +1 V. This process was found to irreversible as a subsequent measurements at 0 V rendered a similar value of μ.

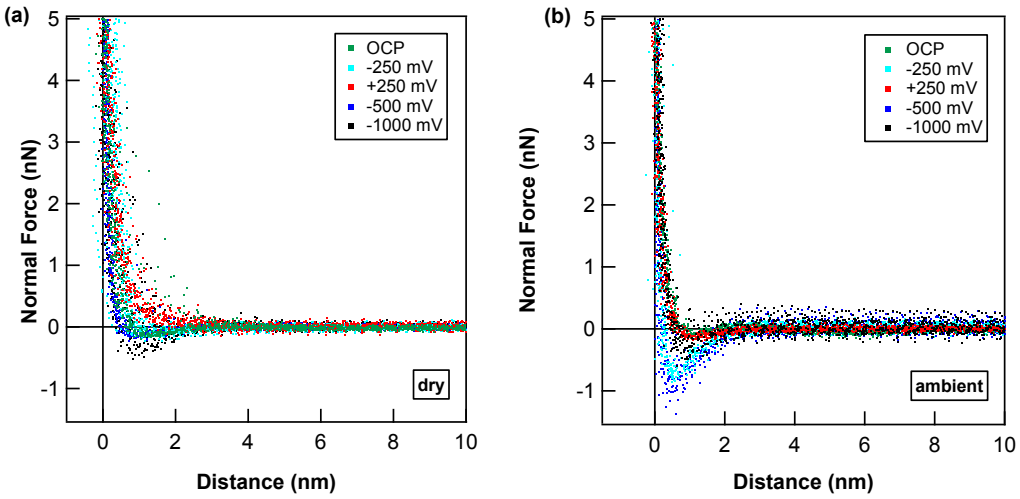


**Fig S7.** AFM normal force-distance curves measured (on approach) between a sharp Si tip and a gold electrode in a 20% w/w solution of $[P_{6,6,6,14}][BMB]$ in PC under **(a)** dry (Argon) and **(b)** ambient conditions (R.H. 22%) at an approach velocity of 1 μm/s.

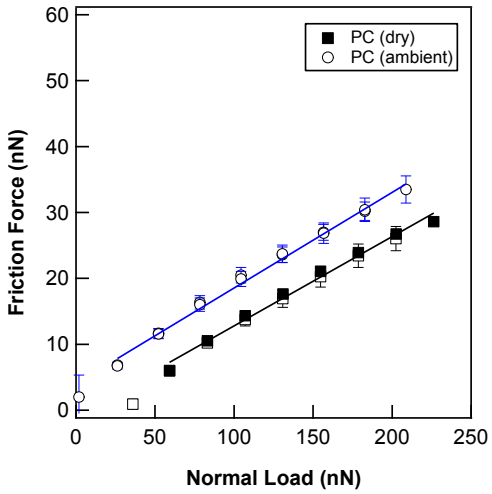


**Fig. S8.** Friction force as a function of normal force measured in pure PC on a gold electrode surface in dry (squares) and ambient (circles) conditions upon loading (closed symbols) and unloading (open symbols) at a velocity of 6 μm/s. The solid and dashed lines represent the linear fits to loading datasets used obtain corresponding friction coefficients for dry and ambient conditions, respectively. For both dry and ambient conditions, the friction coefficient was found to be comparable, with an average value $\mu = 0.14 \pm 0.001$, although the overall friction force was higher in ambient conditions for a given load. The latter is attributed to a more attractive interaction between the tip and the surface occurring in the ambient solution, which causes the surfaces to come into contact at a lower normal load than in the dry IL solution.